Load Aware Self-Organising User-Centric Dynamic CoMP Clustering for 5G Networks

SELCUK BASSOY, MONA JABER, MUHAMMAD ALI IMRAN, (Senior Member, IEEE), AND PEI XIAO

Institute for Communication Systems, University of Surrey, Guildford GU2 7XH, U.K.

Corresponding author: S. Bassoy (s.bassoy@surrey.ac.uk)

ABSTRACT Coordinated multi-point (CoMP) is a key feature for mitigating inter-cell interference, improve system throughput, and cell edge performance. However, CoMP implementation requires complex beamforming/scheduling design, increased backhaul bandwidth, additional pilot overhead, and precise synchronization. Cooperation needs to be limited to a few cells only due to this imposed overhead and complexity. Hence, small CoMP clusters will need to be formed in the network. In this paper, we first present a self-organizing, user-centric CoMP clustering algorithm in a control/data plane separation architecture, proposed for 5G to maximize spectral efficiency (SE) for a given maximum cluster size. We further utilize this clustering algorithm and introduce a novel two-stage re-clustering algorithm to reduce high load on cells in hotspot areas and improve user satisfaction. Stage-1 of the algorithm utilizes maximum cluster size metric to introduce additional capacity in the system. A novel re-clustering algorithm is introduced in stage-2 to distribute load from highly loaded cells to neighboring cells with less load for multi-user joint transmission CoMP case. We show that unsatisfied users due to high load can be significantly reduced with minimal impact on SE.

INDEX TERMS Cooperative communication, mobile communication, clustering algorithms, cellular networks.

I. INTRODUCTION

CoMP or network multiple-input multiple-output (MIMO) is an emerging technology, proposed to reduce interference, hence improve high data rate footprint and cell edge throughput especially in densely deployed, interference limited networks. CoMP has been introduced for long term evolution advanced (LTE-A) by the third generation partnership project (3GPP) in release 11 [1] and it is likely to be a key feature for 5G [2].

The CoMP technology makes use of the shared data between coordinating transmission points (TPs) i.e. channel state information (CSI), scheduling and user data. Inter-cell interference is mitigated or even exploited as useful signal at the receiver. Coordination between all cells in the network is very complex due to the precise synchronisation requirement within coordinated cells, additional pilot overhead, additional signal processing, complex beamforming design and scheduling among all base stations (BSs). It will require high bandwidth backhaul links due to CSI and/or user data exchange between all BSs [3], [4]. In order to reduce this overhead, smaller size cooperation clusters are

required so that coordination only takes place within the cluster. Cluster size should be kept to the optimum levels and dynamically changed based on channel conditions and user profiles. Too small clusters will fail to provide full achievable gains from CoMP. On the other hand, big cluster size will lead to increased overhead on CSI exchange and backhaul capacity requirements [5]. Increased cluster size will give better weighted sum rate [6] but at the cost of additional signal processing and increased feedback and signalling. Furthermore, increased cluster size can lead to energy inefficiency in terms of achieved bits/joule [7].

Optimum cluster selection for cooperation is key for maximising the benefits of CoMP. Static clustering based on a fixed topology is unable to deliver expected gains for future networks as the network topology will be dynamically changing with on/off sleeping cells, user deployed cells with unknown location. Additionally, spatio-temporal distribution of users and service demand will also dynamically change. To maximise CoMP gains, clustering algorithms need to be able to accurately respond to these dynamically changing network conditions and user profiles. Self-organised CoMP

clustering algorithms are required to form dynamically changing optimum clusters by analysing instantaneous network data. Recently emerging self-organising network (SON) platform can be utilised for employing dynamic CoMP clustering algorithms. Data from various sources within the cellular network can be exploited as an input for SON platform. This allows for more accurate dynamic CoMP clustering algorithms, maximising the performance metrics like SE, energy efficiency and load balancing while keeping the fairness between the users [8]. For further reading on SON, an extensive survey is presented in [9].

Dynamic clustering can be classified in three groups based on network elements considered for clustering:

1) **Network-Centric Clustering:** In network-centric clustering approach, cells are clustered in groups where all user equipments (UEs) within the serving area of the clustered cells are served by all cells or a sub-group of cells in the cluster. It is less complex when compared to user-centric clustering, especially from scheduling point of view. However UEs at cluster edge suffer from inter-cluster interference.

2) **User-Centric Clustering:** UEs are allocated their own cluster of cells individually in user-centric clustering approach. Although this method can give better signal-to-interference-plus-noise (SINR) gains, it requires higher backhaul capacity and is more complex, especially in terms of scheduling and precoding design where UE clusters overlap with each other. To reduce complexity, user-centric clustering can be implemented in small groups of cells rather than the whole network.

3) **Hybrid Clustering:** Hybrid clustering approach is the combination of network and user-centric approaches where UEs are allocated their own preferred cells but limited to a bigger group of cells which can dynamically change to adapt to changing network conditions. Hybrid clustering is driven from the complexity/throughput gain trade-off where user-centric clustering is used for better throughput but its complexity is kept at manageable levels by introducing network-centric clustering where UEs are limited to select cells only within the network-centric cluster.

The goal of this paper is to design a load-aware user-centric clustering algorithm within a limited group of cells. We first develop a self-organising, user-centric CoMP clustering algorithm, maximising SE for a given maximum cluster size. We then further develop this clustering algorithm for load awareness and present a novel re-clustering algorithm in two stages. In stage-1, maximum cluster size is allowed to increase further for highly loaded cells to introduce more capacity in the system. A novel re-clustering algorithm is presented in stage-2 to distribute traffic from highly loaded cells to lightly loaded neighbours for MU JT-CoMP case. The trade-off between SE and load balancing is analysed.

The rest of the paper is organised as follows. In Section II, we discuss the load balancing problem and present existing literature. Our system model is presented in Section III.

Our dynamic user-centric clustering algorithm is presented in Section IV. We further enhance the our user-centric clustering in Section V and introduce a re-clustering algorithm to take load balancing into account to distribute the load evenly to unloaded cells. In Section VI, we present results from our simulation and Section VII concludes our work with the outcome and further discussion. Table 1 provides the notation used in this paper.

II. PROBLEM FORMULATION AND PREVIOUS RESEARCH

Mobile network operators experience an exponential increase in mobile data traffic, a 74% increase in 2015 and another 8-fold increase is expected until 2020 [10]. A further 1000-fold capacity increase is projected for the next decade for 5G [2]. Given the very high capacity requirement, load balancing becomes even more important in future cellular networks. Various load balancing schemes have already been studied in the literature [11] for traditional networks. A mathematical framework for cell load and a simple load balancing algorithm is presented in [12]. The authors propose to shift traffic from loaded cell to its unloaded neighbours by changing the handover offset parameter in iterations. In [13], the authors present a distributed, self-organised load balancing algorithm to reduce reference signal power for the congested cell to make neighbour cells more favourable and hence distribute the traffic onto neighbour cells. Another distributed SON algorithm in [14] focuses on BS antenna tilt optimisation to improve SE at hotspots by finding the users' centre of gravity and focusing the antenna beam to the hotspots. The authors in [15] present a distributed load balancing solution from the idea of each BS periodically sharing its average load with UEs. Load information is used along with signal quality to make the decision for cell association. A class of user association schemes for heterogeneous cellular network (HetNet) is presented in [16] to achieve load balancing between macro and small cell layer.

Despite numerous studies for load balancing for traditional networks, there is no study in the literature to our knowledge which explores CoMP clustering with the aim of improving load balancing, although a number of objective functions for CoMP clustering like SE [17]–[21], energy efficiency [7], [22], [23] and backhaul optimisation [24]–[27] have been studied. A novel load-aware, user-centric, dynamic CoMP clustering algorithm is presented in this work where clustering takes load balancing into account to distribute load from congested cells to its less loaded neighbours.

We consider CDSA model which is a recently emerging radio access network (RAN) architecture proposed for 5G networks where macro base stations (MBSs) are used to provide coverage and handle most of the control signalling and small cells (SCs) under the MBSs provide the required data services [28]. We consider that MBSs are enhanced with a CoMP control unit (CCU) and each MBS is connected to all SCs within it's coverage area with fiber backhaul links as illustrated in Figure 1. CCU on the MBS can be deployed within the SON framework and provide intelligent cluster-
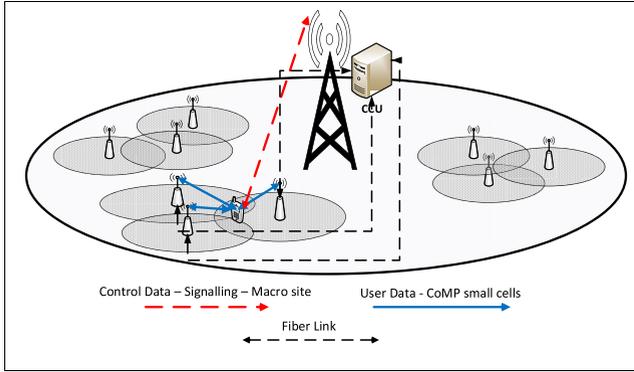
FIGURE 1. Control-Data Separation Architecture.

TABLE 1. Notation.

	Notation used in the paper
$\mathcal{M}$	Set of all small cells
$\mathcal{K}$	Set of all active UEs
$\mathcal{C}_K^k$	Set of UEs scheduled in UE_k's cluster
$\mathcal{C}_M^k$	Set of SCs in UE_k's cluster
$\mathcal{S}_K^m$	Set of active UEs associated with SC_m
g_{km}	Channel coefficient scalar between SC_m to UE_k
$\mathbf{h}_k$	Channel vector for UE_k
w_{mk}	Precoding scalar on SC_m for UE_k
$\mathbf{w}_k$	Precoding vector for UE_k
P_{Tx}	Total transmit power for any SC
P_{km}^{rx}	Received power on UE_k from SC_m
P_{km}^{tx}	Transmit power on SC_m allocated for UE_k
λ_M	PPP SC density
$\lambda_{K_{high}}$	PPP UE density in high traffic area
$\lambda_{K_{low}}$	PPP UE density in low traffic area
R_{tot}	Total number of PRBs for any SC
B_{tot}	Total system bandwidth
B_{RB}	One PRB bandwidth

ing decisions centrally within the SC layer. We assume that CCU also handles central precoding design and baseband processing based on the selected clusters. With all SCs connected to the associated MBS, there is no need for high bandwidth backhaul between the SCs. In addition to CDSA model, our presented algorithm can also be implemented in Cloud-RAN architecture [29], [30] where the clustering decision, precoding, scheduling functions can take place at the "cloud" centrally.

III. SYSTEM MODEL

The system consists of one MBS with M SCs and K users distributed within its coverage area. The SCs are connected to the MBS through optical fibre backhaul links and share their respective CSI data with the MBS. Global precoding is designed and scheduling is performed for all SCs at the CCU located at the MBS. It is assumed that each network layer has exclusive access to a designated frequency spectrum, hence no inter-layer interference is expected between MBS and SCs. Similar designated frequency approach for each layer is also employed in 3GPP LTE-A HetNet deployment scenario [31]. We employ different time-scales for pre-coding and clustering tasks. Precoding is calculated at much faster

rate in response to the fast fading channel conditions, however clustering decisions are updated in longer time intervals based on averaged receive power levels, eliminating fast fading effects [32]–[34]. This gives extra resilience to the clustering algorithm for imperfect CSI knowledge and reduces additional signalling required for more frequent cluster changes [35].

User-centric clustering is employed in this work, where each UE is assigned its own cluster within the group of SCs connected to the same MBS. MU JT-CoMP is employed where user data is available at all SCs within the cluster. Ideal backhaul and perfect CSI knowledge are assumed. Zero forcing (ZF) precoding is employed where intra-cluster interference is completely cancelled. Total transmit power P_{Tx} from each SC is assumed to be equal.

Assume UE_k is assigned a cluster of C_M^k SCs where $|C_M^k| = T$. A group of UEs including UE_k are scheduled at the same physical resource block (PRB) in this cluster. Total number of UEs served at the same time in the cluster is $|C_K^k| = R$. Each UE and SC are assumed to have 1 TP only for simplicity. Group of SCs in C_M^k and the UEs in C_K^k form a *TxR* virtual MIMO system as depicted in Figure 2.
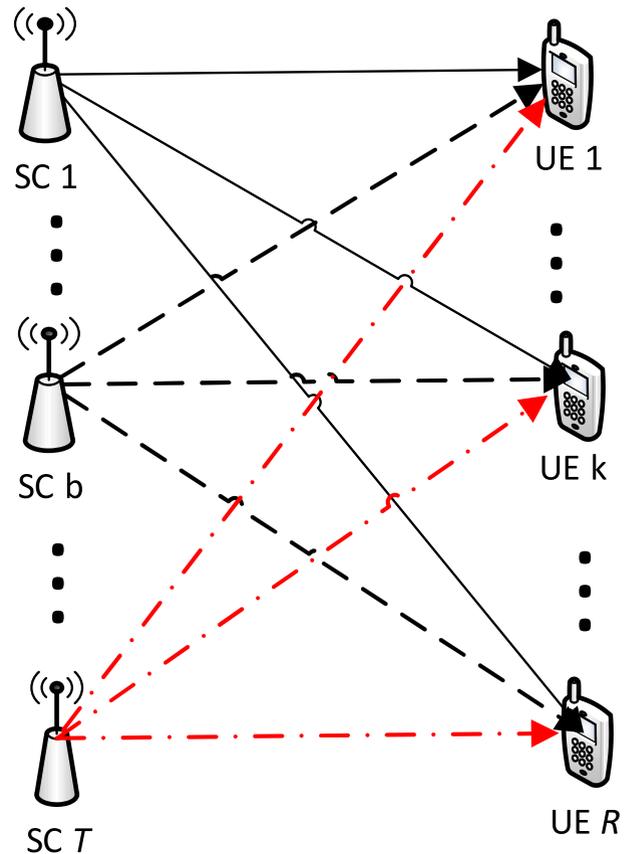

FIGURE 2. Downlink MU JT-CoMP System Model.

Received signal for each UE in C_K^k can be expressed as:

$$\mathbf{y} = \mathbf{HWx} + \mathbf{n}, \ \mathbf{H} \in \mathbb{C}^{R \times M}, \ \mathbf{W} \in \mathbb{C}^{T \times R} \qquad (1)$$

Channel vector at UE_k is expressed as:

$$\mathbf{h}_k = \begin{bmatrix} h_{k1} h_{k2} \dots h_{kT} \end{bmatrix} \tag{2}$$

where $\mathbf{H} = \begin{bmatrix} \mathbf{h}_1 \mathbf{h}_2 \dots \mathbf{h}_R \end{bmatrix}^T$

Beamforming vector for UE_k is expressed as:

$$\mathbf{w}_k = \begin{bmatrix} w_{1k} w_{2k} \dots w_{Tk} \end{bmatrix}^T \tag{3}$$

where $\mathbf{W} = \begin{bmatrix} \mathbf{w}_1 \mathbf{w}_2 \dots \mathbf{w}_R \end{bmatrix}$

Received signal at UE_k can be expressed as:

$$y_k = \mathbf{h}_k^{\mathcal{C}_M^k} \mathbf{w}_k^{\mathcal{C}_M^k} x_k + \sum_{i \in \mathcal{C}_K^k/k} \mathbf{h}_k^{\mathcal{C}_M^k} \mathbf{w}_i^{\mathcal{C}_M^k} x_i + \sum_{j \in \mathcal{K}/C_K^k} \mathbf{h}_k^{\mathcal{M}/\mathcal{C}_M^k} \mathbf{w}_j x_j + n_k \tag{4}$$

First term in (4) represents the desired signal, followed by intra-cluster interference from SCs within the cluster $\mathcal{C}_M^k$ and the third term represents inter-cluster interference from all SCs outside the cluster. Last term n_k represents the additive gaussian white noise (AGWN).

SINR at UE_k can be written as:

$$SINR_k = \frac{|\mathbf{h}_k^{\mathcal{C}_M^k} \mathbf{w}_k^{\mathcal{C}_M^k} x_k|^2}{|\sum_{i \in \mathcal{C}_K^k/k} \mathbf{h}_k^{\mathcal{C}_M^k} \mathbf{w}_i^{\mathcal{C}_M^k} x_i|^2 + |\sum_{j \in \mathcal{K}/C_K^k} \mathbf{h}_k^{\mathcal{M}/\mathcal{C}_M^k} \mathbf{w}_j x_j|^2 + |n_k|^2} \tag{5}$$

We assume perfect channel knowledge and equal transmit power for all PRBs within the SC. Also equal total transmission power (P_{Tx}) is assumed for all SCs. Zero forcing precoder is employed at the CCU. Intra-cluster interference term cancels out with zero forcing precoder and with equal transmision power (P_{Tx}) from each SC. Consequently, (5) can be simplified to:

$$\hat{SINR}_k = \frac{P_{Tx} \sum_{i \in \mathcal{C}_M^k} |h_{ki}|^2}{P_{Tx} \sum_{j \in \mathcal{M}/\mathcal{C}_M^k} |h_{kj}|^2 + N_0 B_{tot}} \tag{6}$$

where N_0 is the noise spectral density and B_{tot} is the total system bandwidth. Channel coefficient h_{ki} is made up of 2 terms, static distance based path loss component with shadow fading and fast fading complex coefficients:

$$h_{ki} = g_{ki} f_{ki} \tag{7}$$

In (7), g_{ki} is the distance based path-loss and shadow fading component and f_{ki} is the complex fast fading channel coefficient. As discussed earlier, clustering decisions are proposed to be based on long term received power levels, hence the fast fading component in (6) is averaged out. Consequently, (6) can be further simplified to eliminate fast fading component for clustering decisions:

$$\hat{SINR}_k = \frac{P_{Tx} \sum_{i \in \mathcal{C}_M^k} |g_{ki}|^2}{P_{Tx} \sum_{j \in \mathcal{M}/\mathcal{C}_M^k} |g_{kj}|^2 + N_0 B_{tot}} \tag{8}$$

IV. USER-CENTRIC CLUSTERING ALGORITHM

We consider user-centric clustering where each UE_k has its own cluster based on the average received power levels. All UEs report their average received reference signal power levels from each of the SCs to their best serving SC. Reported signal levels from each UE are sent from the serving SC to the CCU located at the MBS through the fiber backhaul.

CCU process this information and assign an SC cluster to each UE for cooperation. We propose to limit the complexity of user-centric clustering by keeping the clustering only to the SCs which are connected to the same MBS. This approach can also be considered as a hybrid approach where all SCs connected to the same MBS form a network-centric cluster and user-centric clustering is employed within the network-centric cluster. Management of inter-cluster interference between the SCs which are connected to different MBSs is out of scope for this work. Cluster size is designed to dynamically change for each UE_k, based on received power levels. SCs within closer range of the serving SC's received power level are included in the cluster and a minimum power threshold is applied to avoid including SCs with lower received power levels in the clusters unnecessarily.

The proposed user-centric clustering algorithm works as follows:

1) For each UE_k, the average received power levels from all SCs within the MBS are known at the CCU. Received power levels will be averaged in time, eliminating the fast fading component. Hence g_{km} in (9) consists of path loss and shadow fading only, i.e.,

$$P_{km}^{rx} = P_{km}^{tx} |g_{km}|^2, m \in \mathcal{M} \tag{9}$$

where P_{km}^{tx} is the transmit power allocated for UE_k at SC_m. P_{km}^{rx} is the average received power at UE_k from SC_m

2) P_{km}^{rx} is sorted for each UE_k.

$$\mathcal{P}_{km}^{rx} = \arg \max_m P_{km}^{rx}, m \in \mathcal{M} \tag{10}$$

P_{k1}^{rx} is the received power from serving SC for UE_k. Similarly P_{k2}^{rx} indicates the received power from 2nd best serving SC and so on.

3) Choose cluster $\mathcal{C}_M^k$ for UE_k from SCs with highest received power levels with the following conditions:

  a) Number of SCs in $\mathcal{C}_M^k$ don't exceed the maximum cluster size defined for the algorithm. This is a tunable input parameter to the algorithm where complexity against CoMP efficiency trade-off can be balanced.

$$|\mathcal{C}_M^k| \leq MaxClusterSize \tag{11}$$

  b) Received power level P_{km}^{rx} should not be lower than a minimum threshold. This ensures that SCs which don't provide sufficient coverage to UE_k are not added to the cluster, preventing increased signalling and wasted resources without significant CoMP gains.

$$P_{km}^{rx} > P_{min}^{rx} \tag{12}$$

  c) Received power level of the SCs should also meet a relative power margin criteria for adding to UE_k cluster. This ensures that only the SCs within a

similar received power range to the serving SC are included in the cluster.

$$P_{km}^{rx}/P_{k1}^{rx} > P_{margin} \tag{13}$$

V. CLUSTERING WITH LOAD BALANCING

Next, we discuss how to utilise user-centric clustering algorithm defined in the previous section and propose a novel load balancing algorithm to dynamically change clusters to distribute load evenly in hotspot areas. In the following subsection, we define cell load and unsatisfied users metrics for user-centric CoMP clustering scenario. Then, the clustering algorithm with load balancing is detailed in subsection V-B.

A. CELL LOAD AND UNSATISFIED USERS METRIC

In [12], a mathematical framework is developed for cell load for traditional networks and a term called "unsatisfied users" is introduced for UEs with available throughput below the guaranteed bit rate for their service. Based on this work, we derive the cell load and unsatisfied users metrics for MU JT-CoMP scenario. Our proposed CoMP clustering algorithm will aim to minimise the total number of unsatisfied users in the system.

Each SC is assumed to have R_{tot} allocated PRBs where each PRB has a bandwidth of B_{RB}. Based on the Shannon capacity formula, the maximum achievable throughput from one PRB can be estimated as:

$$y_k = B_{RB}log_2(1 + S I \hat{N} R_k) \tag{14}$$

We assume that constant bit rate d_k is required for each user UE_k, hence the average number of required PRBs for each user for no CoMP scenario can be expressed as: $r_k^{NoCoMP} = d_k/y_k$. But in the MU-JT CoMP case, user data for UE_k is also transmitted from the other SCs in the cluster $\mathcal{C}_M^k$. So, UE_k requires resources from each of the SCs in its cluster. On the other hand, same resources allocated for UE_k are shared with other UEs $\in C_K^k$ which are scheduled in the same cluster. We assume the number of UEs sharing the same PRB in the same cluster is equal to the the cluster size for UE_k i.e., $|C_M^k| = |C_K^k| = n_k$. Hence, average number of "virtually" dedicated PRBs for UE_k will be $r_k^{CoMP} = r_k/n_k$. Virtually dedicated PRBs required for UE_k from all SCs in the $\mathcal{C}_M^k$ cluster can be defined as:

$$r_k = \frac{d_k}{y_k n_k} \tag{15}$$

For example, assume a cluster of three SCs with three UEs scheduled at the same time, on the same PRB from each of the SCs in the cluster. The PRB requirement for each UE from each SC is 1/3, and hence the total number of PRB requirements for all three SCs adds up to three, i.e., one PRB from each SC.

Let $\mathcal{S}_K^m$ be the associated active UE list in SC_m. $s_m = |\mathcal{S}_K^m|$ is the number of UEs associated with SC_m. Load on SC_m (l_m) can be defined as the proportion of the number of used

PRBs to the total number of PRBs on SC_m. Since load can not exceed one, l_m can be expressed as:

$$l_m = \min\left(1, \frac{\sum_{k\in\mathcal{S}_K^m} r_k}{R_{tot}}\right) \tag{16}$$

From l_m in (16), we can also define virtual SC load $\hat{l}_m$ which is allowed to go beyond one, and give a measure of the overload on SC_m:

$$\hat{l}_m = \frac{\sum_{k\in\mathcal{S}_K^m} r_k}{R_{tot}} \tag{17}$$

From (17), we can define an "unsatisfied users" term to indicate the load on the SC. Given that, all users are assumed to require constant bit rate d_k, the users are defined as "satisfied" if they obtain the required bit rate, otherwise unsatisfied. For example, when $\hat{l}_m \leq 1$, all associated users are satisfied in SC_m and when load increases to $\hat{l}_m = 4$, only one fourth of the users are satisfied [12].

To be able to calculate unsatisfied users for each SC for a given load, we need to express a virtual dedicated UE association for each SC where UEs are associated with one SC only. As defined above, $\mathcal{S}_K^m$ represents the active UE list in SC_m, however UEs are associated to multiple SCs in the MU-JT CoMP case. Since each UE is repeated on all SCs in its cluster, virtual dedicated UE association in each SC can be found by adding up all associated UEs with a factor of $1/n_k$ i.e its cluster size. Virtual number of UEs associated with each SC can be expressed as:

$$\hat{s}_m = \sum_{k\in\mathcal{S}_K^m} \frac{1}{n_k} \tag{18}$$

Consequently, the number of unsatisfied users on SC_m can be defined as:

$$u_m = \max\left(0, \hat{s}_m\left(1 - \frac{1}{\hat{l}_m}\right)\right) \tag{19}$$

B. CLUSTERING ALGORITHM WITH LOAD BALANCING

User-centric clustering algorithm discussed in Section IV is further enhanced in this section to balance the load across the SCs and hence to minimise the number of unsatisfied users.

Clustering for load balancing is designed in 2 stages:

1) **Stage-1: Increase maximum cluster size:** Increased cluster size provides additional capacity in a given cluster with MU JT-CoMP at the expense of additional complexity as discussed in Section I. In the proposed algorithm, the capacity/complexity trade-off is managed by a tunable maximum cluster size limit for low and high load scenarios separately. The allowed maximum cluster size is incremented for UEs associated with overloaded SCs in every iteration. SC load is monitored at each iteration to make sure that the cluster size is not increased unnecessarily to the maximum limit when overload is cleared. This part of the algorithm is further explained in stages below and a flow chart is provided in Figure 3a.
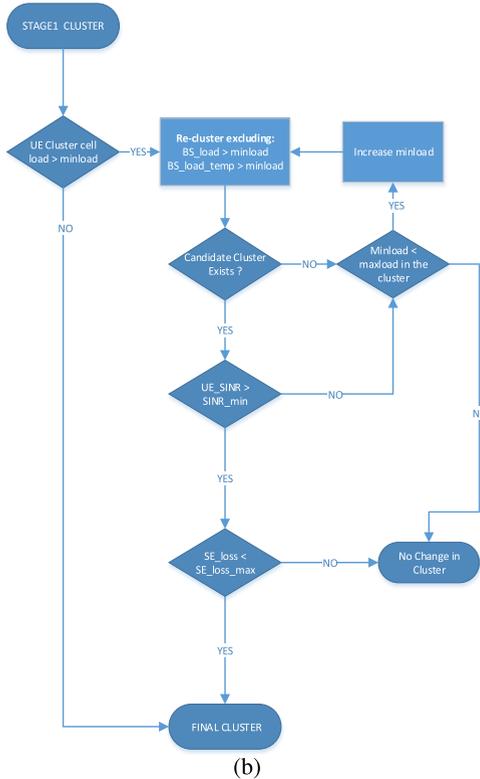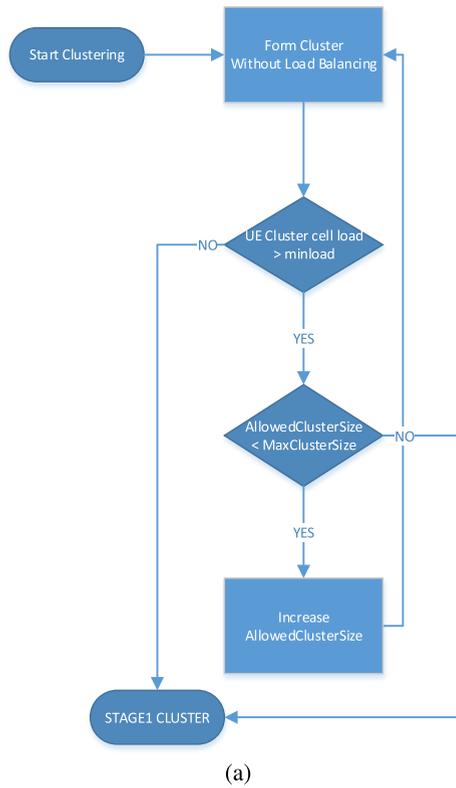
FIGURE 3. Clustering with Load Balancing Algorithm. (a) Stage-1. (b) Stage-2.

a) Identify UEs which have any SCs in its cluster where $l_m > load_{min}$.
b) Increment the maximum allowed cluster size by one, and re-cluster all UEs identified above.

While UEs are re-clustered, new SC loads are computed, and UE list with highly loaded SCs is also updated.

c) Above 2 steps are repeated until:
   i) There is no loaded SCs left OR
   ii) Maximum cluster size is reached

2) **Stage-2: Re-cluster excluding overloaded SCs:**
   After stage-1 of the algorithm, if there are still UEs which have any SCs in its cluster where $l_m > load_{min}$, then stage-2 kicks off to distribute load from highly loaded cells to neighbour cells with light load. This part of the algorithm is further explained below and a flow chart is given in Figure 3b.

   a) Form new candidate cluster excluding SCs where $l_m > load_{min}$, and calculate estimated load for each SC in the candidate cluster. Remove any SCs if $l_m^{estimated} > load_{min}$ and re-cluster again until a candidate cluster is found.
   b) If such cluster exists where $l_m < load_{min}$ and $l_m^{estimated} < load_{min}$, then check if $SINR_k > SINR_{min}$
   c) If $SINR_k > SINR_{min}$, then calculate estimated SE of the candidate cluster and check SE loss when compared to the current cluster SE.
   d) If $SEloss < MaxAllowedSELoss$, then change cluster and recalculate new SC load.
   e) If there is no candidate cluster available which meets the $load_{min}$ or $SINR_{min}$ criteria, then increase the $load_{min}$ parameter in stages and repeat above steps to form a candidate cluster.

   All UEs which include a highly loaded SC in their cluster are checked with above Stage-2 algorithm and re-clustered if a candidate cluster is available for a given max SE loss limit. If there are still highly loaded SCs after the first iteration, Stage-2 algorithm is repeated for more iterations with increased $MaxAllowedSELoss$ at each iteration until high load is cleared on all SCs. This assures minimal impact on SE loss, i.e., UEs at the cell edge of the loaded SCs will be handed over to less loaded SCs first and gradually UEs closer to the loaded cell center are re-clustered in further iterations if required.

VI. NUMERICAL RESULTS

In order to evaluate the proposed CoMP clustering scheme, one MBS is considered and its coverage is approximated with a circle of 0.4km radius; SCs are distributed randomly over the MBS coverage area. To simulate the unplanned nature of SC deployment in future cellular networks, SCs are modelled as random network (RN) following poisson point process (PPP) distribution with density parameter λ_M. UEs are also randomly distributed following PPP distribution with density $\lambda_{K_{high}}$ and $\lambda_{K_{low}}$. MBS coverage area is assumed to have uneven traffic distribution where there is high user density $\lambda_{K_{high}}$ within the inner circle and low user density $\lambda_{K_{low}}$ in the outer ring. SCs deployed within the inner circle will be

highly loaded and the aim is to reduce the load on these SCs by shifting traffic from highly loaded SCs to under-utilised SCs by dynamic CoMP clustering. The radius of the area with high and low user density are assumed to be 0.1km and 0.2km respectively. SCs are deployed within a larger area ($R_B = 0.4km$) to avoid border effect and make sure UEs at the border receive interference from within 0.2km outside the UE radius. The simulation setup with network topology is illustrated in Figure 4.
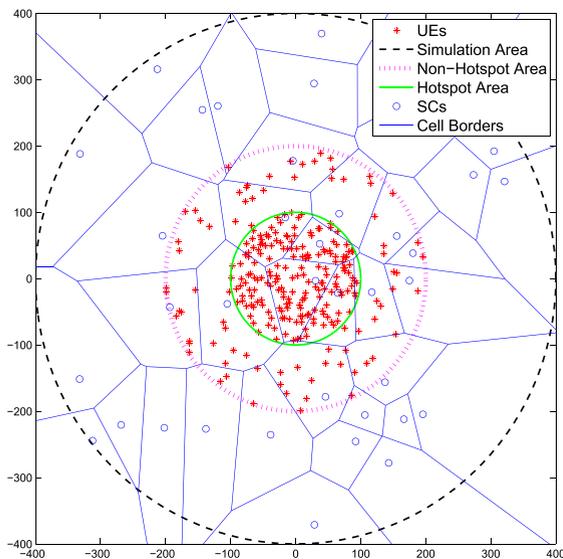

FIGURE 4. Simulation Network Topology Illustration, SC and UE locations, Hotspot and Non-Hotspot areas, SC Borders following Voronoi tessellation.

Each SC is assumed to have one cell with omnidirectional antenna. The ITU-R microcell urban non-line-of-sight (NLOS) path loss model is employed as given in (20) [36].

$$PL = 36.7 \log_{10}(d) + 22.7 + 26 \log_{10}(fc) \qquad (20)$$

Antenna bore-sight gain is assumed to be 17dBi and TP noise figure including the cable loss is assumed to 5dBm as suggested for ITU-R microcell urban test environment [36]. MU JT-CoMP with coherent combining is employed, however proposed algorithm can be easily adapted to other coordination methods i.e. single user (SU) JT-CoMP or coordinated scheduling/beam-forming. The rest of the simulation parameters are provided in Table 2.

A. COMPLEXITY OF THE PROPOSED ALGORITHM

Before we present the numerical results from our simulation, the complexity of our proposed solution is evaluated in this subsection: Our proposed algorithm employs a user-centric clustering approach to maximise CoMP gains and it increases cluster size gradually to utilise the additional capacity for highly loaded cells. Furthermore, a re-clustering algorithm is proposed to shift UEs from loaded cells into relatively less-loaded cells. User-centric clustering provides better CoMP gains, however implementing such design

TABLE 2. Simulation parameters.

Parameter Name	Parameter Value
Simulation Enviroment	Urban Microcell [36]
Frequency Carrier	5 Ghz
Channel Bandwidth	5 Mhz
RB Bandwith	180kHz
Number of PRBs/SC	25
Shadow fading std	4 dB [36]
UE Antenna Gain	0 dBi
UE Thermal Noise Density	-174 dBm/Hz
TP Total Transmit Power	41dBm [36]
UE Noise Figure	7dB
TP Noise Figure (inc cable loss)	5dB
SC antenna gain (boresight)	17dBi
Min RX Power to include in cluster	-110dBm
Max RX power offset from serving SC	20dB
Min Required SINR	0
Max Cluster Size (no Overload)	3
Max Cluster Size (Overload)	6
Guaranteed bit rate for UEs	512 kbps
SC Density Dense Deployment (λ_M)	80SC/km^2
SC Density Medium Deployment (λ_M)	40SC/km^2
SC Density Sparse Deployment (λ_M)	20SC/km^2
MS Density Hotspot High Load($\lambda_{K_{high}}$)	12000UE/km^2
MS Density Hotspot Medium Load($\lambda_{K_{high}}$)	10000UE/km^2
MS Density Hotspot Low Load($\lambda_{K_{high}}$)	6000UE/km^2
MS Density Non-Hotspot($\lambda_{K_{low}}$)	800UE/km^2
Simulation Area Radius R_B	0.4km
Non-Hotspot Area Radius	0.2km
Hotspot Area Radius	0.1km
Minimum Load	80%

comes with increased complexity due to additional pilot overhead, additional signal processing, complex beamforming and scheduling design. The complexity increases with increased cluster size [3], [4]. In our presented algorithm, we reduce this complexity by introducing a tunable maximum cluster size parameter which can be set separately for users within over-loaded and less-loaded SC coverage areas. Hence a balance between improved spectral efficiency, cell load, user satisfaction and complexity of implementing such design can be tuned based on network structure, traffic demand and backhaul availability etc. Moreover, our proposed algorithm limits the user-centric clustering to the set of SCs within one MBS coverage area in a CDSA architecture. Precoding and scheduling is performed centrally at the MBS and clustering is not allowed between SCs connected to different MBSs to reduce complexity.

A simple approach is followed for both stages of the algorithm to form UE clusters based on the reported average received signal levels and cell load for each SC. CCU at the MBS utilises this data for clustering decisions within longer time intervals eliminating fast fading changes, hence more resilient clustering decisions are achieved in the case of partial CSI availability [35]. However, complexity of the algorithm increases with the number of users within the MBS coverage area, and the number of SCs connected to the MBS. To reduce this complexity, network-centric sub-clusters will need to be deployed for larger MBS coverage areas where presented user-centric clustering algorithm can be deployed within these smaller network-centric clusters. Further research in this area is identified at the conclusion section.
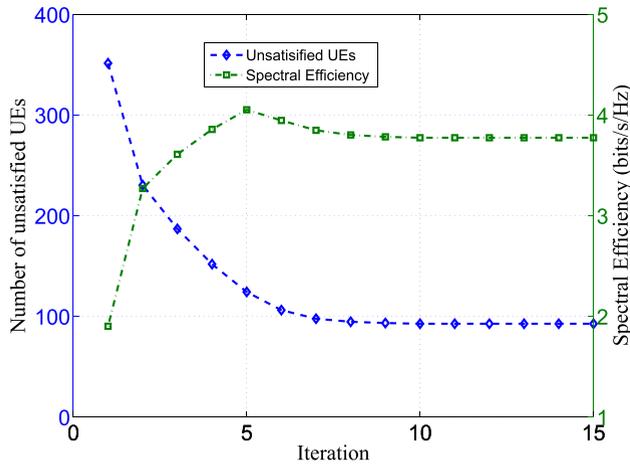
FIGURE 5. Unsatisfied UEs and SE changes for dense deployment scenario with high load.

B. DENSE DEPLOYMENT WITH HIGH LOAD SCENARIO

Figure 5 depicts the changes in the number of unsatisfied users and average SE in iterations for dense network deployment with high UE load case. First iteration shows the unsatisfied users when CoMP is not employed. Our presented user-centric CoMP clustering is employed in the next iteration with maximum cluster size of three without taking SC load into account. This reduces the number of unsatisfied users by 34.4% due to the additional capacity introduced with MU JT-CoMP. Maximum achievable cell throughput at different iteration points is shown in Figure 9. Stage-1 of the load balancing algorithm is employed at the next three iterations where only the UEs attached to highly loaded cells are allowed to increase cluster size beyond the original value of three. Iterations 3,4 and 5 in Figure 5 give the reduction in the number of unsatisfied UEs by increasing maximum cluster size to 4, 5 and 6 respectively. Unsatisfied UEs are reduced by an additional 30.2% at this stage. SE continues to increase as CoMP cluster size increases at this stage. Once cluster size is increased to the maximum limit for loaded cells, then stage-2 of the load balancing algorithm starts to further reduce the unsatisfied users based on re-clustering for UEs which are served by SCs where $CellLoad > load_{min} = 80\%$. UEs are re-clustered only if the SE loss is below a certain threshold at each iteration. This threshold is increased at each iteration until either all UEs are satisfied, or the maximum allowed limit for SE loss threshold is reached. This ensures that UEs located at the cell edge of the loaded SCs are re-clustered to other neighbour SCs first and gradually more UEs are re-clustered until cell load is reduced to $< load_{min} = 80\%$. SE loss steps are set to 1, and max SE loss threshold is set to 5 in this simulation. An additional 9% of the unsatisfied UEs are reduced due to re-clustering in dense deployment case. (i.e iterations 6-15 in Figure 5). Total number of unsatisfied UEs are reduced by 73.6% when compared to no-CoMP case. Re-clustering in stage-2 comes with the cost of reduced SE as some of the UEs served by loaded SCs will be handed over to the non-best serving SCs. 6.84% reduction in SE is observed

when compared to iteration-5 in the dense deployment with high load case. In return for SE loss, more users have been allocated their guaranteed data rates, resulting in the reduction of unsatisfied UEs by 9%. SE distribution at different stages of the algorithm is shown in Figure 6.
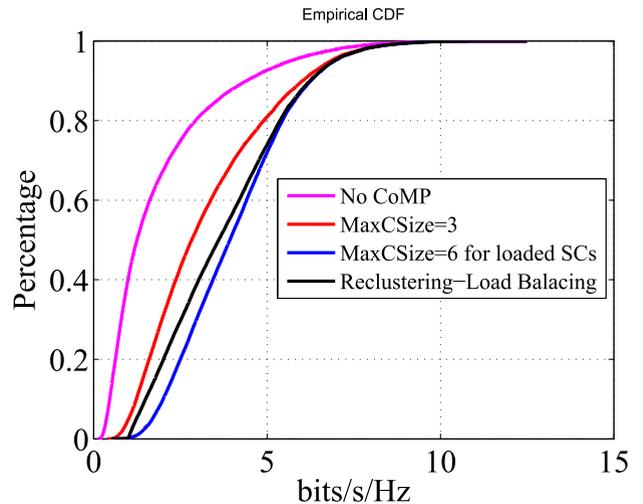

FIGURE 6. SE distribution for dense deployment scenario with high load.

Maximum achievable SC throughput for cluster sizes of 1, 3, 4, 5, 6 and after the stage-2 re-clustering algorithm are shown in Figure 9. Deployment of MU JT-CoMP with cluster size of three (iteration 2) increases the SC throughput by 71.9% when compared to no-CoMP scenario. As the cluster size increases, throughput/SC grows, however the growth rate slows down with higher cluster size as the number of users which can benefit from high cluster size is much less based on the density of SC deployment. Increasing the cluster size from three to six for the loaded cells (stage-1 algorithm - iteration 3-4-5) increases the system throughput by a further 23.9%. However, system throughput is reduced by 6.8% during the stage-2 phase of the algorithm in return for further reducing the unsatisfied users by handing-over some users from loaded best-serving cells to clusters of relatively less loaded cells as explained above. An overall SC throughput gain of 98.4% is achieved when compared to non-CoMP case.

Figure 7 depicts the cluster size distribution at 3 different iteration points, i.e., iterations 2, 5, and 15, which capture the cluster size distribution when maximum cluster size is set to 3, 6, and at the end of the re-clustering iteration, respectively. 86.1% of the UEs had 3 cells in their cluster when the initial clustering algorithm was deployed, however when the cluster size is increased to 6 for load balancing, UEs with maximum cluster size of 6 is reduced to 60.9%. This is due to clustering algorithm not allowing cluster size increase if it's not required for load balancing.

C. DENSE/MEDIUM/SPARSE DEPLOYMENT

Simulations are run for dense/medium/sparse deployment scenarios with 80, 40 and 20 SC/km^2 respectively to compare the effectiveness of the algorithm. Figure 10 shows the
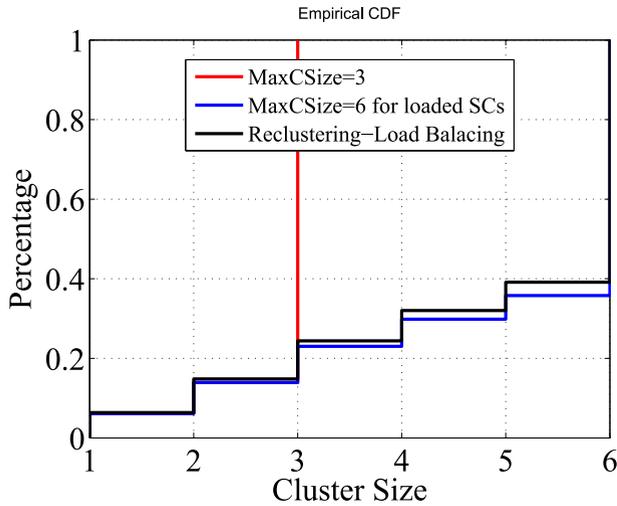
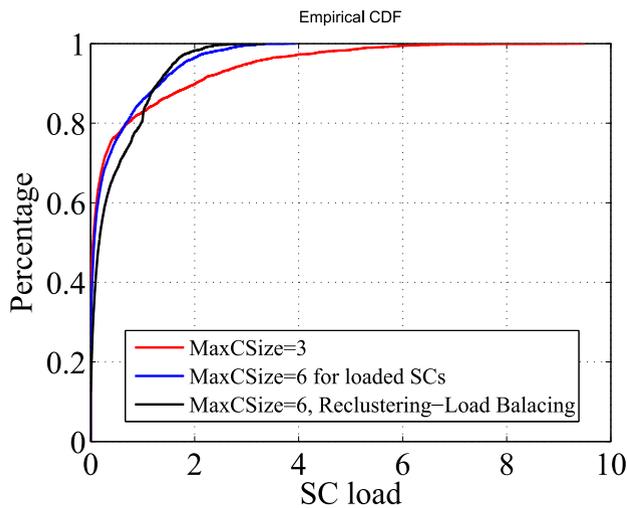**FIGURE 7.** Cluster size distribution for dense deployment scenario with high load.

FIGURE 8. SC load distribution - Dense Deployment scenario with high load.

FIGURE 9. Max Achievable Throughput/SC - Dense Deployment scenario with high load.
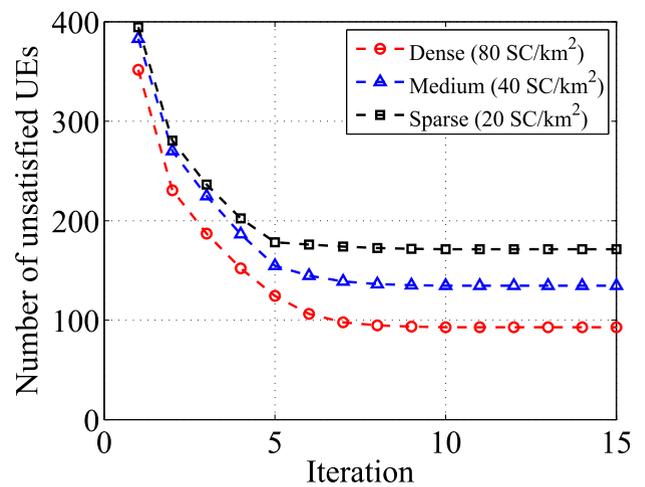
FIGURE 10. Unsatisfied UEs for Dense/Medium/Sparse deployment scenarios with high load.
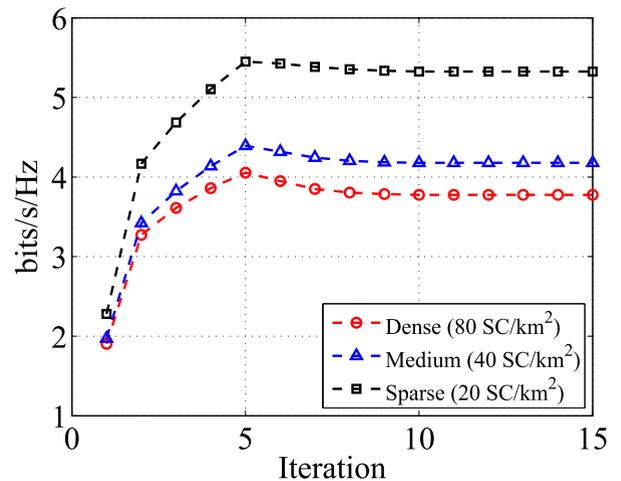
FIGURE 11. Mean SE for Dense/Medium/Sparse deployment scenarios with high load.

unsatisfied UEs reduced by 73.6%, 64.8% and 56.6% for dense, medium and sparse deployment, respectively. Results clearly show that presented algorithm is more effective in the dense deployment scenario. As presented in Figure 12, sparse deployment results in significantly lower cluster size, due to lack of available SCs with overlapping coverage, hence limiting the re-clustering options for load balancing. Figure 13 shows the SC load distribution at sparse deployment scenario where re-clustering is not effective. However, SC load distribution shows a clear improvement in dense deployment scenario due to re-clustering in Figure 8. SE changes are compared in Figure 11 showing negligible SE loss in sparse deployment due to re-clustering not being effective for reasons explained above.

D. DENSE DEPLOYMENT WITH HIGH/ MEDIUM/LOW LOAD

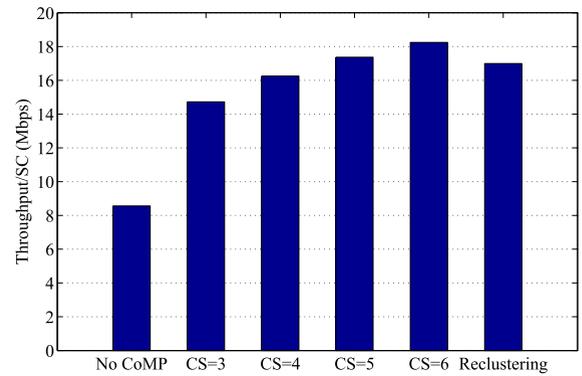Proposed scheme is also evaluated for different UE load conditions. Figure 14 shows the change in unsatisfied UEs

for dense deployment in high/medium/light load scenarios. In the light load scenario, unsatisfied UEs have almost completely cleared at iteration 6, limiting the SE loss allowed for re-clustering to 1 only. Figure 17 shows SC load distribution
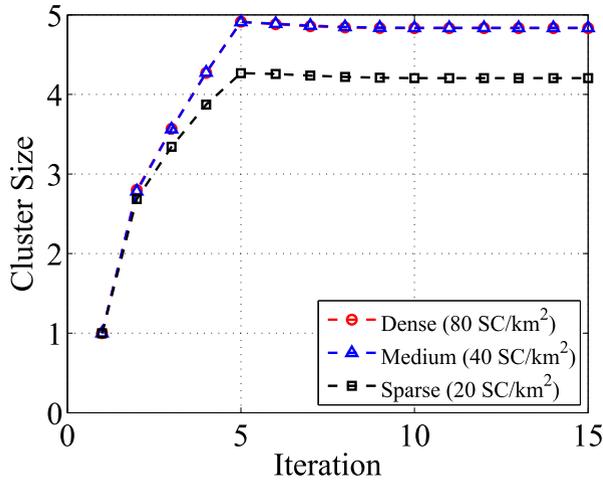
FIGURE 12. Mean Cluster Size for Dense/Medium/Sparse deployment scenarios with high load.
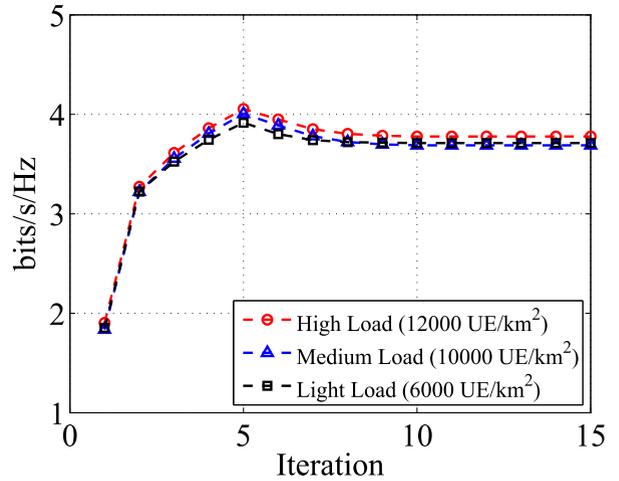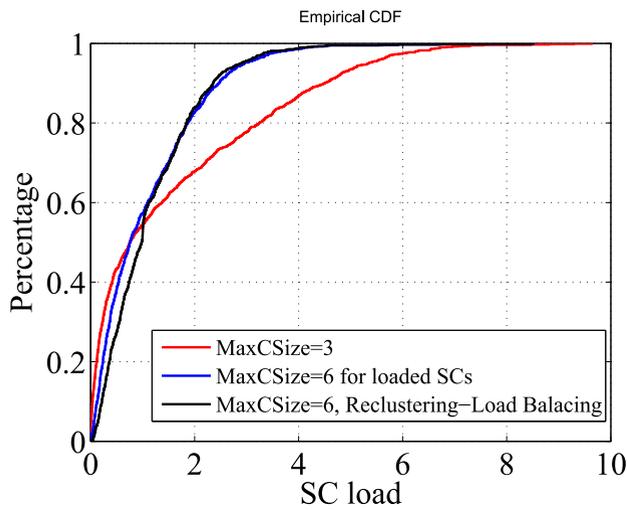

FIGURE 13. SC load distribution - Sparse deployment scenerio with high load.

FIGURE 14. Unsatisfied UEs for Dense deployment scenerio with high/medium/light load.

FIGURE 15. SE for Dense deployment scenerio with high/medium/light load.

FIGURE 16. Cluster size in for Dense deployment scenerio with high/medium/light load.

FIGURE 17. SC load distribution – for Dense deployment scenerio with light load.
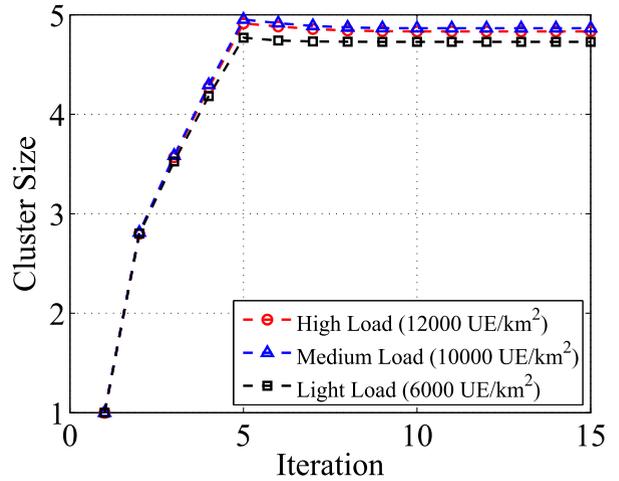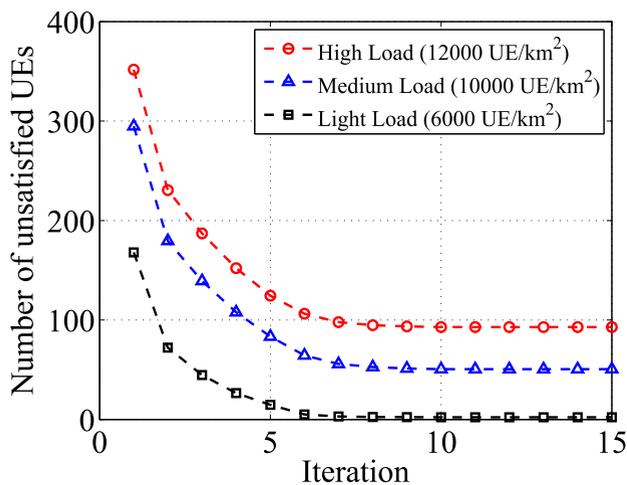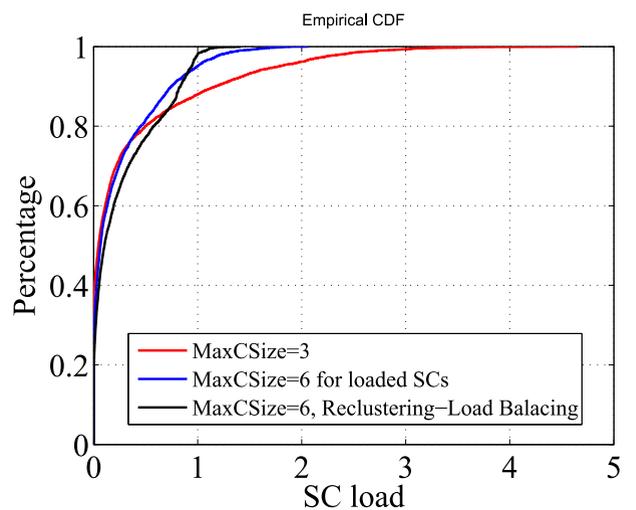
reflecting on the reduction of unsatisfied UEs where almost all SC load is reduced below 1. On the other hand, Figure 16 shows that average cluster size is significantly lower in the

light load scenario. The algorithm is only applied to the UEs served by loaded SCs which is the lower portion of the total UEs for light load case. Lower cluster size has direct
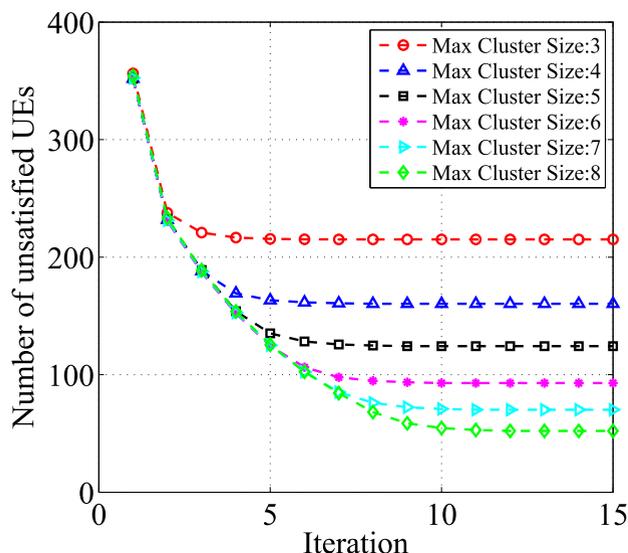
FIGURE 18. Unsatisfied UEs for dense deployment with high load for different max Cluster Size.

effect on SE, hence light load scenario has the lowest SE in Figure 15. On the other hand, SE loss due to re-clustering is minimum in the light load scenario as well, as shown in Figure 15 from iteration 5 to 12.

Finally, Figure 18 shows the total number of unsatisfied UEs for different allowed maximum cluster size in the dense deployment scenario with high load. As the cluster size increases, the impact on reducing the unsatisfied UE metric slows down. Based on the density of the deployment, max cluster size need to be optimised carefully for the right balance between maximising the load balancing gains and increased complexity due to high cluster size.

VII. CONCLUSION

A novel load-aware, user-centric CoMP clustering is presented in this paper. It is shown that additional capacity generated by deploying MU JT-CoMP can be utilised for load balancing by increasing the cluster size when required. Increased complexity with cluster size can be reduced by employing proposed algorithm only when it is required for load balancing. It's also shown that maximum allowed cluster size should be selected carefully based on the SC density, as larger cluster size has minimal impact in relatively sparse deployment scenario. Furthermore, we present a novel re-clustering algorithm which distributes the traffic from highly loaded cells to neighbour cells with light load, reducing the number of unsatisfied UEs significantly. SE loss is minimised by re-clustering in iterations, starting from the UEs at the cell edge first and move closer to the cell center until overload is cleared. In light load scenario, overload is cleared in early iterations, hence SE loss and maximum cluster size is kept low. Furthermore, it is shown that presented algorithm is most effective in dense deployment scenario which is the likely case for CoMP deployment in future 5G networks.

Complexity of employing user-centric clustering is limited to the coverage area of one MBS in the proposed algorithm. However, depending on the SC density, increased complexity may require a further network-centric clustering algorithm to limit the group of SCs for cooperation. Furthermore, network-centric clustering can also be employed for cooperation between multiple MBSs to eliminate interference between SCs connected to different MBSs. A self-organised, load-aware network-centric CoMP clustering algorithm will be studied in the future to complement this work. Further research is also required to asses backhaul bandwidth constraint and imperfect CSI scenarios. Load balancing need to be combined with other objectives for a more comprehensive multi-objective CoMP clustering algorithm to jointly optimise spectral efficiency, backhaul bandwidth constraint, energy efficiency and load balancing with imperfect CSI.

REFERENCES

[1] 3GPP, "Coordinated multi-point operation for LTE physical layer aspects," 3rd Generat. Partnership Project (3GPP), Tech. Rep. 36.819 R11 v11.2.0, Sep. 2013.

[2] Q. C. Li, H. Niu, A. T. Papathanassiou, and G. Wu, "5G network capacity: Key elements and technologies," *IEEE Veh. Technol. Mag.*, vol. 9, no. 1, pp. 71–78, Mar. 2014.

[3] R. Irmer *et al.*, "Coordinated multipoint: Concepts, performance, and field trial results," *IEEE Commun. Mag.*, vol. 49, no. 2, pp. 102–111, Feb. 2011.

[4] D. Lee *et al.*, "Coordinated multipoint transmission and reception in LTE-advanced: Deployment scenarios and operational challenges," *IEEE Commun. Mag.*, vol. 50, no. 2, pp. 148–155, Feb. 2012.

[5] P. Marsch and G. Fettweis, "Static clustering for cooperative multi-point (CoMP) in mobile communications," in *Proc. IEEE Int. Conf. Commun.*, Jun. 2011, pp. 1–6.

[6] A. S. Rodríguez and A. G. Armada, "Analysis of the cluster size in coordinated multipoint transmission," in *Proc. 19th Signal Process. Commun. Appl. Conf.*, Apr. 2011, pp. 1197–1200.

[7] G. Cili, H. Yanikomeroglu, and F. R. Yu, "Cell switch off technique combined with coordinated multi-point (CoMP) transmission for energy efficiency in beyond-LTE cellular networks," in *Proc. Int. Conf. Commun. (ICC)*, Jun. 2012, pp. 5931–5935.

[8] A. Imran, A. Zoha, and A. Abu-Dayya, "Challenges in 5G: How to empower SON with big data for enabling 5G," *IEEE Netw.*, vol. 28, no. 6, pp. 27–33, Nov. 2014.

[9] O. G. Aliu, A. Imran, M. A. Imran, and B. Evans, "A survey of self organisation in future cellular networks," *IEEE Commun. Surveys Tuts.*, vol. 15, no. 1, pp. 336–361, 1st Quart., 2013.

[10] *Cisco Visual Networking Index: Global Mobile Data Traffic Forecast Update, 2015–2020*, Cisco, San Jose, CA, USA, Feb. 2016.

[11] A. Sharma, A. Roy, S. Ghosal, R. Chaki, and U. Bhattacharya, "Load balancing in cellular network: A review," in *Proc. 3rd Int. Conf. Comput. Commun. Netw. Technol. (ICCCNT)*, Jul. 2012, pp. 1–5.

[12] I. Viering, M. Dottling, and A. Lobinger, "A mathematical perspective of self-optimizing wireless networks," in *Proc. Int. Conf. Commun. (ICC)*, Jun. 2009, pp. 1–6.

[13] A. Imran, E. Yaacoub, M. A. Imran, and R. Tafazolli, "Distributed load balancing through self organisation of cell size in cellular systems," in *Proc. 23rd Int. Symp. Pers. Indoor Mobile Radio Commun. (PIMRC)*, Sep. 2012, pp. 1114–1119.

[14] A. Imran, M. A. Imran, Atta-ul-Quddus, and R. Tafazolli, "Distributed spectral efficiency optimization at hotspots through self organisation of BS tilts," in *Proc. GLOBECOM Workshops*, Dec. 2011, pp. 570–574.

[15] H. Kim, G. de Veciana, X. Yang, and M. Venkatachalam, "α-optimal user association and cell load balancing in wireless networks," in *Proc. IEEE INFOCOM*, Mar. 2010, pp. 1–5.

[16] Q. Ye, B. Rong, Y. Chen, M. Al-Shalash, C. Caramanis, and J. G. Andrews, "User association for load balancing in heterogeneous cellular networks," *IEEE Trans. Wireless Commun.*, vol. 12, no. 6, pp. 2706–2716, Jun. 2013.

[17] J.-M. Moon and D.-H. Cho, "Formation of cooperative cluster for coordinated transmission in multi-cell wireless networks," in *Proc. IEEE 10th Consum. Commun. Netw. Conf. (CCNC)*, Jan. 2013, pp. 528–533.

[18] S. Feng, W. Feng, H. Mao, and J. Lu, "Overlapped clustering for comp transmissions in massively dense wireless networks," in *Proc. IEEE Int. Conf. Commun. Syst. (ICCS)*, Nov. 2014, pp. 308–312.

[19] P. Baracca, F. Boccardi, and V. Braun, "A dynamic joint clustering scheduling algorithm for downlink CoMP systems with limited CSI," in *Proc. Int. Symp. Wireless Commun. Syst. (ISWCS)*, Aug. 2012, pp. 830–834.

[20] J. Zhao, T. Zhang, Z. Zeng, Q. Gao, and S. Sun, "An overlapped clustering scheme of coordinated multi-point transmission for LTE-A systems," in *Proc. IEEE 14th Int. Conf. Commun. Technol. (ICCT)*, Nov. 2012, pp. 479–484.

[21] F. Guidolin, L. Badia, and M. Zorzi, "A distributed clustering algorithm for coordinated multipoint in LTE networks," *IEEE Wireless Commun. Lett.*, vol. 3, no. 5, pp. 517–520, Oct. 2014.

[22] S. Han, C. Yang, G. Wang, and M. Lei, "On the energy efficiency of base station sleeping with multicell cooperative transmission," in *Proc. 22nd Int. Symp. Pers. Indoor Mobile Radio Commun. (PIMRC)*, Sep. 2011, pp. 1536–1540.

[23] D. Cao, S. Zhou, C. Zhang, and Z. Niu, "Energy saving performance comparison of coordinated multi-point transmission and wireless relaying," in *Proc. IEEE Global Telecommun. Conf. (GLOBECOM)*, Dec. 2010, pp. 1–5.

[24] D. Samardzija and H. Huang, "Determining backhaul bandwidth requirements for network MIMO," in *Proc. 17th Eur. Signal Process. Conf. (EUSIPCO)*, Aug. 2009, pp. 1494–1498.

[25] T. Biermann, L. Scalia, C. Choi, H. Karl, and W. Kellerer, "Improving CoMP cluster feasibility by dynamic serving base station reassignment," in *Proc. 22nd Int. Symp. Pers. Indoor Mobile Radio Commun. (PIMRC)*, Sep. 2011, pp. 1325–1330.

[26] J. Zhao and Z. Lei, "Clustering methods for base station cooperation," in *Proc. IEEE Wireless Commun. Netw. Conf. (WCNC)*, Apr. 2012, pp. 946–951.

[27] J. Zhao, T. Q. S. Quek, and Z. Lei, " Semi-distributed clustering method for CoMP with limited backhaul data transfer," in *Proc. IEEE Wireless Commun. Netw. Conf. (WCNC)*, Apr. 2013, pp. 3776–3781.

[28] A. Mohamed, O. Onireti, M. A. Imran, A. Imran, and R. Tafazolli, "Control-data separation architecture for cellular radio access networks: A survey and outlook," *IEEE Commun. Surveys Tuts.*, vol. 18, no. 1, pp. 446–465, 1st Quart., 2015.

[29] *C-RAN: The Road towards Green RAN*, China Mobile, China, 2011.

[30] K. Sundaresan, M. Y. Arslan, S. Singh, S. Rangarajan, and S. V. Krishnamurthy, "FluidNet: A flexible cloud-based radio access network for small cells," in *Proc. 19th Annu. Int. Conf. Mobile Comput. Netw.*, 2013, pp. 99–110.

[31] 3GPP, "Evolved universal terrestrial radio access (E-UTRA); mobility enhancements in heterogeneous networks," Tech. Rep. 36.839, Jun. 2011.

[32] A. Giovanidis, J. Krolikowski, and S. Brueck, "A 0–1 program to form minimum cost clusters in the downlink of cooperating base stations," in *Proc. IEEE Wireless Commun. Netw. Conf. (WCNC)*, Apr. 2012, pp. 940–945.

[33] R. Weber, A. Garavaglia, M. Schulist, S. Brueck, and A. Dekorsy, "Self-organizing adaptive clustering for cooperative multipoint transmission," in *Proc. IEEE 73rd Veh. Technol. Conf. (VTC Spring)*, May 2011, pp. 1–5.

[34] V. Garcia, Y. Zhou, and J. Shi, "Coordinated multipoint transmission in dense cellular networks with user-centric adaptive clustering," *IEEE Trans. Wireless Commun.*, vol. 13, no. 8, pp. 4297–4308, Aug. 2014.

[35] A. Papadogiannis and G. C. Alexandropoulos, "The value of dynamic clustering of base stations for future wireless networks," in *Proc. Int. Conf. Fuzzy Syst. (FUZZ)*, Jul. 2010, pp. 1–6.

[36] *Guidelines for Evaluation of Radio Interface Technologies for IMT-Advanced*, document ITU-R M.2135.1, ITU-R, Geneva, Switzerland, Dec. 2009.

SELCUK BASSOY received the B.E. degree in electrical and electronics engineering from Middle East Technical University (METU), Ankara, Turkey, in 1999. Since 1999, he has been working in the wireless telecommunications industry, providing consultancy on radio access network design, planning, and optimization for global telecommunications companies, such as Ericsson, T-Mobile, Telefonica, and Vodafone. He is currently with Telefonica U.K. Ltd., as a Principal Engineer, specialized in self-organizing networks and other smart automation tools for GSM/UMTS/LTE radio access networks. He is currently pursuing the Ph.D. degree with the 5G Innovation Centre, University of Surrey, researching on 5G radio access network coordination and clustering techniques. His research interests include wireless communications, network MIMO, self-optimization, coordinated multi-point, radio resource management, and load balancing.

MONA JABER received the B.E. degree in computer and communications engineering and the M.E. degree in electrical and computer engineering from the American University of Beirut, Beirut, Lebanon, in 1996 and 2012, respectively. She is currently pursuing the Ph.D. degree with the 5G Innovation Centre, University of Surrey, researching on 5G backhaul solutions. She was a Telecommunication Consultant in various international firms with focus on radio design of cellular networks, including GSM, GPRS, UMTS, and HSPA. Her research interests are wireless communications, cellular technologies, backhaul and fronthaul solutions, and self-optimization techniques.

MUHAMMAD ALI IMRAN (M'03–SM'12) received the M.Sc. (Hons.) and Ph.D. degrees from Imperial College London, London, U.K., in 2002 and 2007, respectively. He is currently a Reader (Associate Professor) with the Institute for Communication Systems, University of Surrey, U.K. He is an Adjunct Associate Professor with the University of Oklahoma. He is leading a number of international research projects encompassing the areas of energy efficiency, fundamental performance limits, sensor networks, and self-organizing cellular networks. He is also leading the new physical layer work area for 5G innovation centre with the University of Surrey. He has a global collaborative research network spanning both academia and key industrial players in the field of wireless communications. He has supervised over 20 successful Ph.D. graduates. He has contributed to ten patents and authored over 150 peer-reviewed research papers, including more than 20 IEEE TRANSACTIONS. He received the IEEE Comsoc's Fred Ellersick Award 2014, the FEPS Learning and Teaching Award 2014, and twice nominated for Tony Jean's Inspirational Teaching Award. He was a shortlisted finalist for The Wharton-QS Stars Awards 2014 for innovative teaching and VC's learning and teaching award at the University of Surrey. He is a Senior Fellow of the Higher Education Academy, U.K.

PEI XIAO received the Ph.D. degree from the Chalmers University of Technology, Sweden, in 2004. Prior to joining the University of Surrey in 2011, he was a Research Fellow with Queen's University, Belfast, and had held positions with Nokia Networks, Finland. He is a Reader with the University of Surrey and also the Technical Manager of the 5G Innovation Centre (5GIC), leading and coordinating research activities, and overseeing major projects in all the work areas with 5GIC. His research interests and expertise span a wide range of areas in communications theory and signal processing for wireless communications. He has published extensively in the field of wireless communications and in the cross-disciplinary areas of DSP and microwave propagation.

● ● ●